WORLD JOURNAL OF PHARMACEUTICAL RESEARCH
Coden USA: WJPRAP Impact Factor 8.63
Volume 15, Issue 14, 1120-1137. Research Article ISSN 2277–7105

ANTIBACTERIAL ACTIVITY, MOLECULAR DOCKING, IN-SILICO ADME, AND TOXICITY STUDIES: SYNTHESIS OF N-(4-NITROBENZYL) ANILINE AND N-(4-NITROBENZYLIDENE) ANILINE

Shailesh S. Gurav[1]*, Seema R. Jadhav[2], Pranaya P. Iswalkar[3]

Department of Chemistry, VIVA College, Virar (W), Maharashtra-401303, India.

Article Received on 15 June 2026,
Article Revised on 05 July 2026,
Article Published on 16 July 2026,
https://doi.org/10.5281/zenodo.21369471

***Corresponding Author**
Shailesh S. Gurav
Department of Chemistry, VIVA College, Virar (W), Maharashtra-401303, India.

How to cite this Article: Shailesh S. Gurav[1]*, Seema R. Jadhav[2], Pranaya P. Iswalkar[3] (2026). Antibacterial Activity, Molecular Docking, In-Silico Adme, And Toxicity Studies: Synthesis of N-(4-Nitrobenzyl) Aniline And N-(4-Nitrobenzylidene) Aniline. World Journal of Pharmaceutical Research, 15(14), 1120–1137.

ABSTRACT

In the present investigation, two compounds, 4-methyl-N-(4-nitrobenzylidene) aniline (**3**) and 4-methyl-N-(4-nitrobenzyl)aniline **(4)**, were successfully synthesized through an efficient synthetic method and obtained in good yields. Synthesized Schiff base was further reduced via $NaBH_4$, and their structures were confirmed by[1] H NMR spectra. Synthesized compounds displayed broad-spectrum antibacterial activity against *Staphylococcus aureus*, *Bacillus subtilis*, *Escherichia coli*, and *Klebsiella pneumoniae* with moderate to good inhibitory effects. Compound **3** showed good antibacterial potency against *S. aureus* (24 mm) and *K. pneumoniae* (20 mm). Further, molecular docking studies against the target protein (PDB ID: 1KZN, E. coli) exhibited good binding affinity (docking scores of -7.7 and -7.4 kcal/mol) with diverse binding interactions with active-site residues. ADME prediction revealed satisfactory pharmacokinetic profiles for both compounds, including high gastrointestinal absorption, BBB permeability, and non-substrate behavior toward P-glycoprotein. Further, zero Lipinski rule violations and a bioavailability score of 0.55, suggesting good oral drug-likeness. Overall, both compounds exhibited promising antibacterial activity, favorable binding interactions, pharmacokinetic and toxicity properties, thus representing promising scaffolds for further study and biological evaluation.

KEYWORDS: 4-methyl-N-(4-nitrobenzyl)aniline, toxicity, antibacterial activity, molecular docking, in-silico ADME.

1. INTRODUCTION

Schiff bases, characterized by the presence of a carbon–nitrogen double bond, represent a vital class of organic compounds synthesized through the condensation of primary amines with carbonyl derivatives.[1,2] These compounds, discovered by Hugo Schiff in 1864, feature an azomethine moiety that facilitates diverse structural coordination and significant pharmacological potential.[3-5] Beyond their utility in coordination chemistry, these derivatives serve as versatile synthons for the synthesis of various heterocycles, including thiazolidines and benzoxazines.[6] The pharmacological profile of these compounds is particularly extensive, as they have demonstrated significant antimicrobial, anti-inflammatory, and antineoplastic efficacy in various clinical research models (**Figure 1)**.[7]

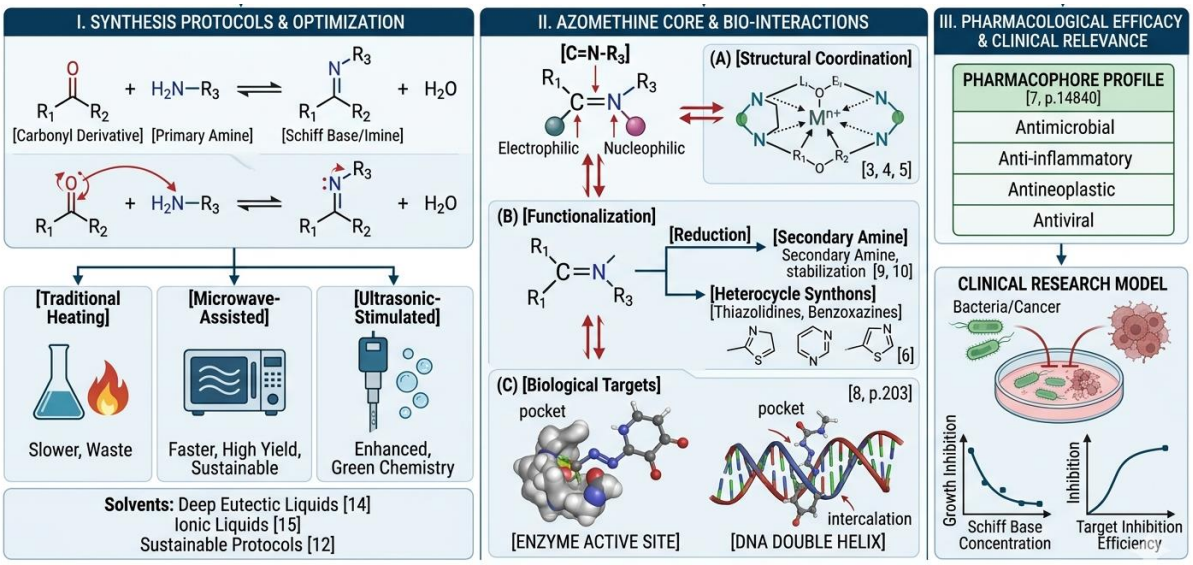

Figure 1: Schiff bases: synthesis, properties, and multifaced applications.

Furthermore, the electrophilic nature of the imine carbon and the nucleophilic nitrogen atom permit effective binding interactions with biological targets, including enzymes and DNA, thereby inhibiting pathological replication processes.[8] The reduction of the azomethine linkage to secondary amines represents a crucial strategy for stabilizing these structures and modifying their pharmacokinetic profiles.[9,10] Subsequent synthesis techniques—ranging from microwave-assisted irradiation to ultrasonic stimulation—have further optimized the yields of these scaffolds while enabling more sustainable protocols.[11-15] These advancements are particularly critical when functionalizing the resulting amine derivatives for enhanced

interaction with transition metals, thereby optimizing the biological potency of the metal-ligand scaffold.[16, 17]

Moreover, the subsequent reduction of the azomethine linkage to form secondary amines often serves to modulate the lipophilicity and metabolic stability of these pharmacophores, facilitating more effective target site localization.[5, 9] Also, recent investigations emphasize the capacity of these transition metal complexes to function as potent urease inhibitors, offering a pathway for developing therapeutics with improved bioavailability and safety profiles.[18-20] Some complexes also exhibit significant potential in the development of optoelectronic devices, including organic photovoltaic cells and light-activatable inorganic therapeutic agents, through photoinduced electron transfer mechanisms.[21-22] The integration of mechanochemical and sonochemical methods alongside these refined synthetic routes further facilitates the development of sustainable, high-purity production frameworks for complex heterocyclic architectures.[23-24] Furthermore, the flexi-dentate nature of these ligands allows for selective coordination. Such structural adaptability is particularly advantageous in medicinal chemistry, as it allows these complexes to engage with biological targets that enhance their cytotoxicity against tumor cells.[25] The integration of these Schiff base metal complexes into therapeutic regimens has demonstrated broad-spectrum efficacy, specifically exhibiting potent antifungal, antibacterial, and antiproliferative properties.[26] These diverse bioactivities stem largely from the molecule's superior chelating capability, which facilitates the formation of stable complexes with transition metals that mimic the active sites of biological enzymes.[27, 28] With this consideration in mind, we decided to synthesize 4-methyl-N-(4-nitrobenzylidene)aniline and 4-methyl-N-(4-nitrobenzyl)aniline and screen these compounds for their antibacterial activity. And further study their binding interactions, ADME properties, toxicity via molecular docking, pharmacokinetics, and toxicity evaluations.

2. MATERIALS AND METHODS

2.1 Chemicals, and equipment

For all experiments, we used chemicals obtained from Loba Chemicals, India. The prepared silica gel TLC plates were used to monitor the progress of reactions. All melting points were recorded in open capillary tubes and are uncorrected. ^{1}H NMR spectra were recorded on an Avance Neo 500 instrument in $CDCl_3$ at 500 MHz. Biological activity was obtained from the Aakar-Biotech laboratory.

2.2 *In-vitro* biological screening methods

The antimicrobial susceptibility testing was done by the agar well-diffusion method as described by the agar well diffusion method (Perez *et al.*, 1990).

2.3 Computational methods

2.3.1 Molecular docking studies: The protein and ligand preparation, grid generation, and docking were executed using AutoDockTools 1.5.6 software.[37] The stable conformation of molecules was obtained by geometry optimization utilizing the Chem3D Pro 12 program. A known Protein Database Bank (https://www.rcsb.org/) was used to retrieve 3D-crystal structures of protein with PDB ID: 1KZN. 2D and 3D ligand-receptor interactions were analyzed using Discovery Studio visualizer software.[29-31]

2.3.2 *In silico* Pharmacokinetics, ADME, and toxicity studies

The ADME and pharmacokinetic profile of synthesized compounds are determined by using the tool, Swiss ADME. Toxicity prediction of synthesized compounds is obtained by the ProTox-3.0 tool.

3. Synthesis

3.1. Synthesis of 4-methyl-N-(4-nitrobenzylidene)aniline (3)

In a round bottom flask equipped with condenser, the mixture of *p*-nitro benzaldehyde (2.0 g, 13.23 mmol) and *p*-toluidine (1.41 g, 13.32 mmol) in ethanol (10 mL) was added at room temperature (**Reaction scheme 1**). The resulting solution was then refluxed with stirring on hot plate for 4 h. After the completion of reaction (TLC, PET ether: EtOAc), resulting solution was cooled and poured into ice-cold water, which resulted in the precipitation of the corresponding aldimine intermediate, 4-methyl-N-(4-nitrobenzylidene)aniline (**3**) with 87% yield (2.78 g).

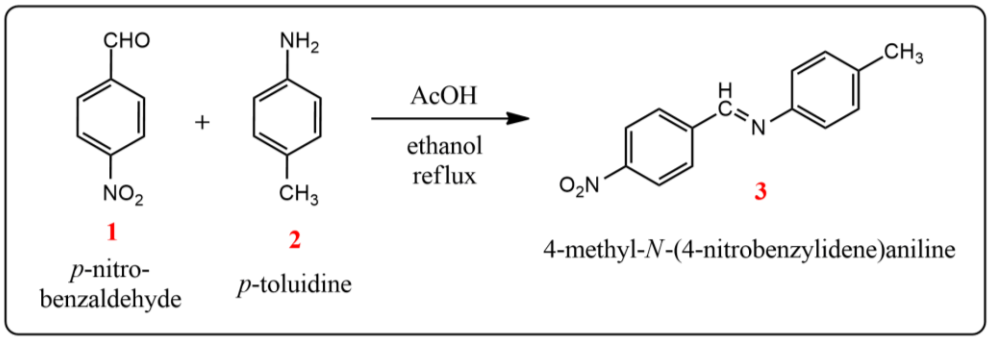

Reaction scheme 1: Synthesis of 4-methyl-N-(4-nitrobenzylidene)aniline**(3).**

3.2. Synthesis of 4-methyl-N-(4-nitrobenzyl)aniline(4)

In a two-neck round-bottom flask connected with the condenser, 4-methyl-N-(4-nitrobenzylidene)aniline (2.0 g, 8.32 mmol) was dissolved in methanol (10 mL). Few drops of AcOH were added to the reaction solution, followed by $NaBH_4$ (0.31 g, 8.32 mmol) at room temperature (**Reaction scheme 2**). The reaction mixture was stirred for 4 h at reflux temperature. After completion of reaction (TLC, PET ether: chloroform, 8:2), reaction mixture was quenched with sat. $NaHCO_3$ solution, extracted with EtOAc (2×15 mL), and concentrated. The resulting crude amine compound was crystallized in ethanol to afford the title compound **(4)** with 73% (1.48 g) yield.

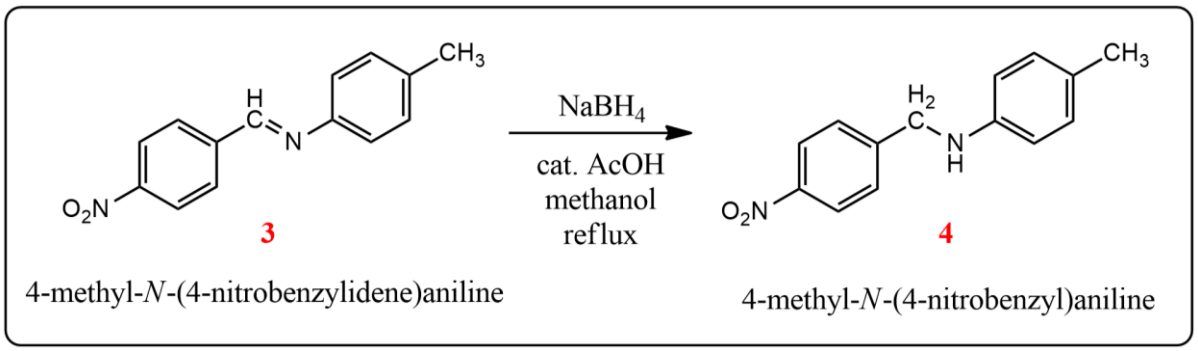

Reaction scheme 2: Synthesis of 4-methyl-N-(4-nitrobenzyl)aniline **(4)**

3.3. Characterization data

3.3.1. 4-methyl-N-(4-nitrobenzylidene)aniline (3)

Greenish-yellow solid, yield: 87.42 %, melting point: 141°C.

^{1}H NMR (500 MHz, $CDCl_3$) δ ppm: 8.56 (s, 1H, CH=N), 8.31-8.29 (d, 2H, ArH), 8.06-8.05 (d, 2H, ArH), 7.24 (d, 2H, ArH), 6.98-6.96 (d, 2H, ArH), 2.23 (s, 3H, CH_3). **MS** (m/z): $C_{14}H_{12}N_2O_2$, 240.03 (M^+).

3.3.2. 4-methyl-N-(4-nitrobenzyl)aniline (4)

Yellow solid, yield: 73.38 %, melting point: 156°C. **^{1}H NMR** (500 MHz, $CDCl_3$) δ ppm: 8.18-8.15 (d, 2H, ArH), 7.53-7.50 (d, 2H, ArH), 6.98-6.95 (d, 2H, ArH), 6.52-6.49 (d, 2H, ArH), 4.44 (s, 2H, CH_2), 4.02 (s, 1H, NH), 2.23 (s, 3H, CH_3). **MS** (m/z): $C_{14}H_{14}N_2O_2$, 240.18 (M^+).

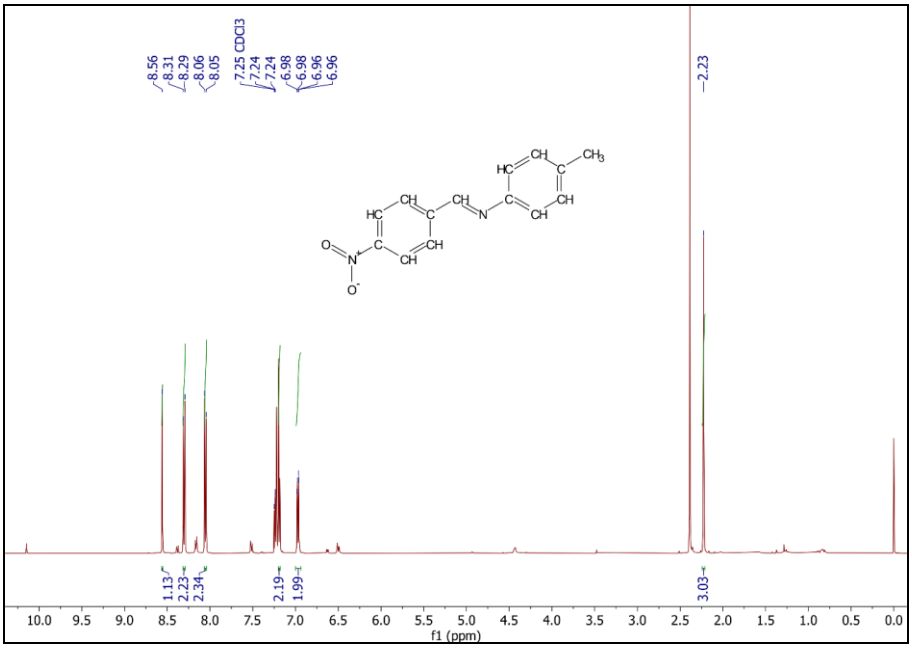

Figure 2: ^{1}H NMR spectra of 4-methyl-N-(4-nitrobenzylidene)aniline (3).

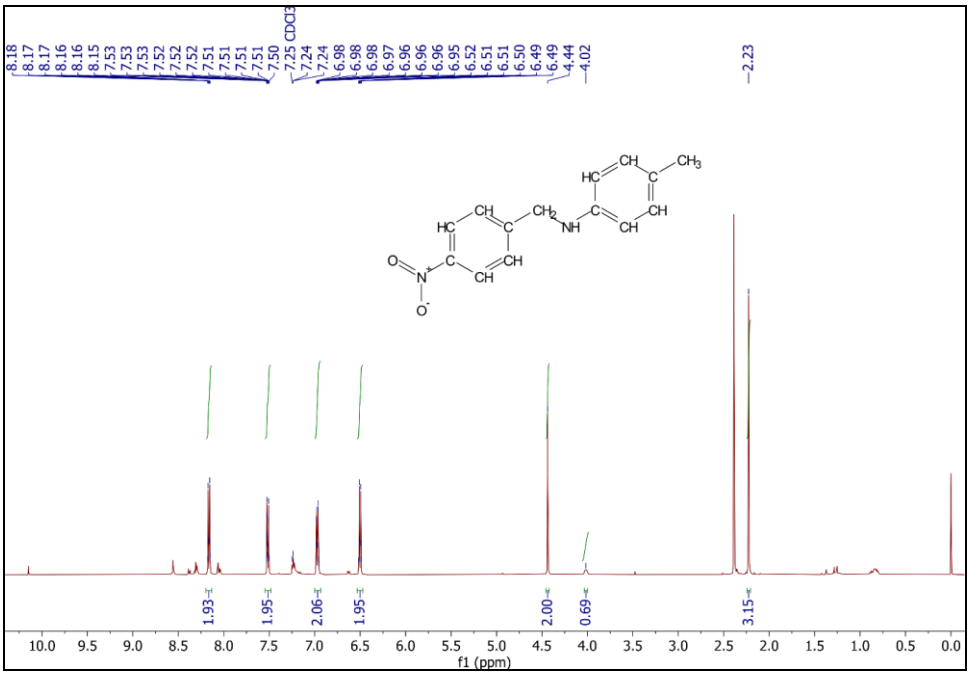

Figure 3: ^{1}H NMR spectra of 4-methyl-N-(4-nitrobenzyl)aniline (4).

4. RESULTS AND DISCUSSION

4.1 Chemistry

Initially, the condensation of *p*-nitrobenzaldehyde (**1**) with *p*-toluidine (**2**) was carried out in the presence of a catalytic amount of acetic acid to obtain aldimine intermediate, 4-methyl-N-(4-nitrobenzylidene)aniline (**3**). Further, the reduction of azomethine (C=N) group of 4-

methyl-N-(4-nitrobenzylidene)aniline (**3**) was achieved via sodium borohydride ($NaBH_4$) in methanol to produce a title compound 4-methyl-N-(4-nitrobenzyl)aniline (**4**) in good yield.

Compound **3**, 4-methyl-*N*-(4-nitrobenzylidene)aniline, was obtained as a greenish-yellow solid in a good yield of 87.42% with a melting point of 141 °C. The structure of the synthesized Schiff base was confirmed by ^{1}H-NMR spectroscopy (**Figure 2**). The characteristic singlet observed at δ 8.56 ppm corresponding to one proton was assigned to the azomethine (–CH=N–) group, confirming successful condensation between the aldehyde and amine precursors. The aromatic protons of the *p*-nitrophenyl ring resonated as two doublets at δ 8.31–8.29 ppm (2H) and δ 8.06–8.05 ppm (2H), reflecting the deshielding influence of the strongly electron-withdrawing nitro substituent. The aromatic protons of the *p*-tolyl ring appeared as two doublets at δ 7.24 ppm (2H) and δ 6.98–6.96 ppm (2H), consistent with a para-substituted aromatic system. Furthermore, the methyl group attached to the tolyl ring gave a distinct singlet at δ 2.23 ppm integrating for three protons. The observed spectral data were in good agreement with the proposed structure of compound **3**, thereby confirming the successful synthesis of the desired Schiff base.

Compound **4**, 4-methyl-*N*-(4-nitrobenzyl)aniline, was isolated as a yellow solid in 73.38% yield with a melting point of 156 °C. The structure of the synthesized secondary amine was confirmed by 1H NMR spectroscopy (**Figure 3**). The aromatic protons of the *p*-nitrobenzyl moiety appeared as two doublets at δ 8.18–8.15 ppm (2H) and δ 7.53–7.50 ppm (2H), attributable to the de-shielding effect of the electron-withdrawing nitro substituent. Similarly, the aromatic protons of the *p*-tolyl ring resonated as two doublets at δ 6.98–6.95 ppm (2H) and δ 6.52–6.49 ppm (2H), consistent with a para-substituted aromatic system. The methylene bridge connecting the two aromatic rings was observed as a singlet at δ 4.44 ppm, integrating for two protons, confirming the presence of the –CH_2–NH– linkage. A singlet at δ 4.02 ppm, corresponding to one proton, was assigned to the secondary amine (–NH–) proton. Furthermore, the methyl group attached to the tolyl ring appeared as a singlet at δ 2.23 ppm, integrating for three protons.

The observed spectral features, particularly the disappearance of the azomethine proton and the appearance of the methylene and amine proton signals, confirmed the successful reduction of the corresponding Schiff base (**3**) to the desired secondary amine, thereby confirming the structure of compound **4**.

4.2 Biological activity: Antibacterial activity

The antibacterial activity of synthesized compounds **3** and **4** was evaluated against two Gram-positive (*Staphylococcus aureus* and *Bacillus subtilis*) and two Gram-negative (*Escherichia coli* and *Klebsiella pneumoniae*) bacterial strains using the zone of inhibition assay, with ciprofloxacin as the standard drug (**Table 1**)[32-33] Compound **3** exhibited the highest activity against *S. aureus* (24 mm) and *K. pneumoniae* (20 mm), while showing moderate inhibition against *E. coli* (15 mm) **(Figure 4**) and *B. subtilis* (12 mm). In contrast, compound **4** demonstrated better activity against *E. coli* (18 mm) and *B. subtilis* (13 mm), with inhibition zones of 21 mm against *S. aureus* and 16 mm against *K. pneumoniae*. Although both compounds displayed broad-spectrum antibacterial activity, their inhibitory effects were lower than those of the standard drug ciprofloxacin (16–30 mm). Overall, compound **3** showed good antibacterial potency compared to compound **4**, particularly against *S. aureus* and *K. pneumoniae*, indicating its potential as a promising antibacterial lead for further investigation.

Table 1: Antibacterial activity (zone of inhibition) of synthesized compounds.

Compound/ Standard	Zone of inhibition (mm)*			
	Gram (+) bacteria		Gram (−) bacteria	
	S. aureus	***B. subtilis***	***E. Coli***	***K. pneumoniae***
3	24	12	15	20
4	21	13	18	16
Ciprofloxacin	28	16	30	26

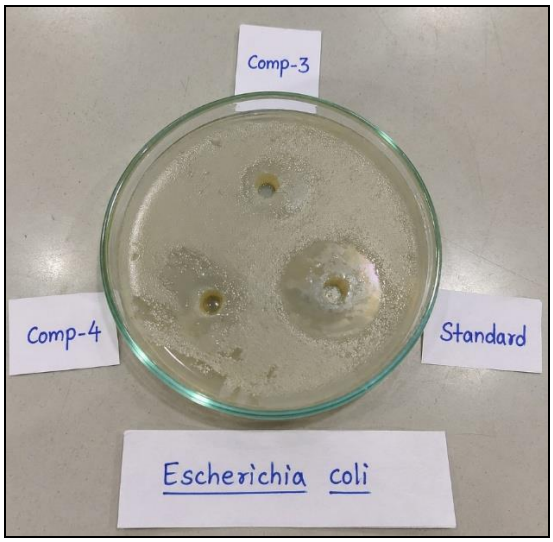

Figure 4: Antibacterial activity (zone of inhibition) of synthesized compounds 3, 4 and standard ciprofloxacin.

4.3. Molecular docking study

Compound **3** (*4-methyl-N-(4-nitrobenzylidene)aniline*) exhibited a docking score of -7.4 kcal/mol with target protein of *E. Coli* (PDB id: 1KZN) (**Table 2**). Based on the 2D interaction diagram of the 1KZN (*E. coli*)–Compound **3** docking complex, the ligand is stabilized within the active site through a combination of conventional hydrogen bonding, π-anion, π-sigma, alkyl, and π-alkyl interactions. A strong conventional hydrogen bond is formed between ARG A:76 and the nitro-group oxygen of the ligand with a bond distance of 2.72 Å, indicating a significant contribution to ligand anchoring (**Figure 5**). The nitro-phenyl ring of the ligand establishes a π-anion interaction with GLU A:50 at a distance of 3.72 Å. In addition, THR A:165 participates in a π-sigma interaction with the aromatic π-system of the ligand, exhibiting an interaction distance of 3.77 Å. Several hydrophobic interactions further stabilize the docked conformation. ILE A:78 forms a π-alkyl interaction with the ligand at 5.09 Å, while ALA A:47 exhibits both alkyl and π-alkyl interactions with distances of 4.09 Å and 5.02 Å, respectively. Likewise, VAL A:71 and VAL A:43 contribute alkyl interactions at distances of 4.15 Å and 4.43 Å, respectively. Another hydrophobic alkyl interaction is observed with VAL A:167 at a distance of 4.09 Å. Collectively, the presence of one strong hydrogen bond, one π-anion interaction, one π-sigma interaction, and multiple hydrophobic alkyl/π-alkyl contacts suggests that Compound **3** is favorably accommodated within the active site of 1KZN, thereby contributing to the stability of the ligand–protein complex.

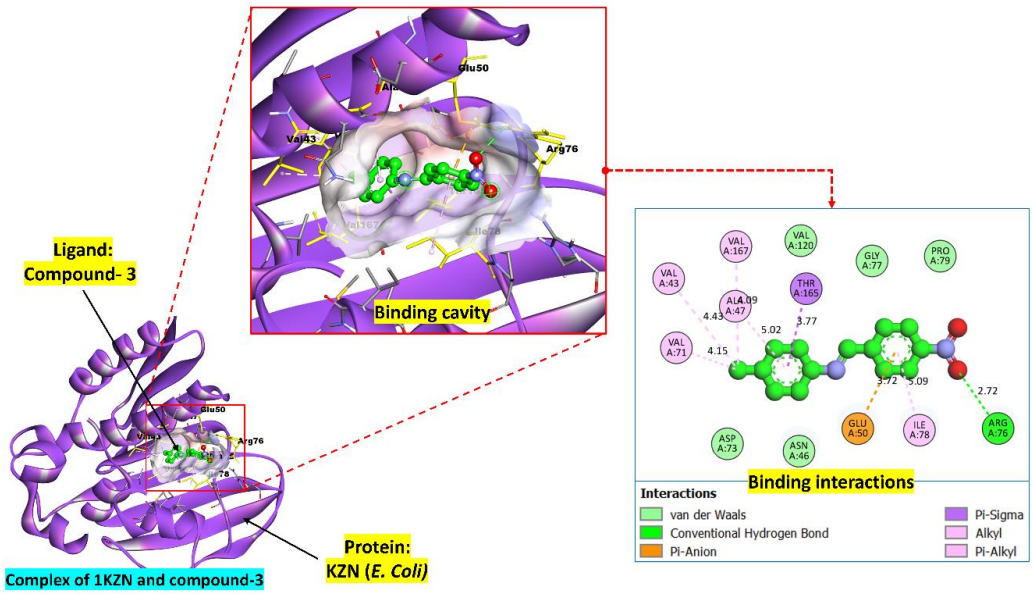

Figure 5: Binding of compound-3 with a target protein 1KZN: binding complex, binding cavity and binding interactions.

Table 2: Binding affinities of compounds against the target protein 1KZN selected for docking.

Compound/ standard	**Target protein** (PDB ID) **1KZN (*E. coli*) Binding energy (kcal/mol)**
5a	-7.4
5b	-7.7
ciprofloxacin	-8.9

Similarly, compound **4** (*4-methyl-N-(4-nitrobenzyl)aniline*) exhibited a docking score of -7.7 kcal/mol with target protein of *E. Coli* (PDB id: 1KZN). The docking analysis of compound **4** with 1KZN (*E. coli*) revealed that the ligand is stabilized within the active site through a combination of hydrogen bonding, π-based interactions, alkyl/π-alkyl contacts, and van der Waals forces (**Figure 6**). Two conventional hydrogen bonds were observed between the ligand (**4**) and ARG A:76 and ARG A:136 at distances of 2.85 Å and 6.49 Å, respectively, involving the nitro-group oxygen of the ligand and contributing to strong anchoring within the binding pocket. In addition, a carbon–hydrogen bond was formed with ASN A:46 at 3.53 Å, further stabilizing the ligand orientation. The aromatic system of the ligand engaged in a π–sigma interaction with THR A:165 at 3.90 Å, while a π–anion interaction was observed with GLU A:50 at 3.72 Å. Several hydrophobic interactions also contributed to binding affinity. VAL A:167 exhibited a π–alkyl interaction at 4.26 Å, whereas VAL A:71, ASP A:73, ALA A:47, and VAL A:43 formed alkyl interactions at distances of 4.26 Å, 4.89 Å, 5.24 Å, and 4.89 Å, respectively. Another π–alkyl interaction was detected with ILE A:78 at 5.09 Å. Residues such as VAL A:120, GLY A:77, PRO A:79, and MET A:91 mainly contributed through van der Waals contacts, helping to maintain the ligand in an optimal binding conformation. Overall, the presence of strong hydrogen bonds, π–anion interaction, π–sigma contact, and multiple hydrophobic interactions suggests that Compound 4 is favorably accommodated within the active site of 1KZN, resulting in a stable ligand–protein complex.

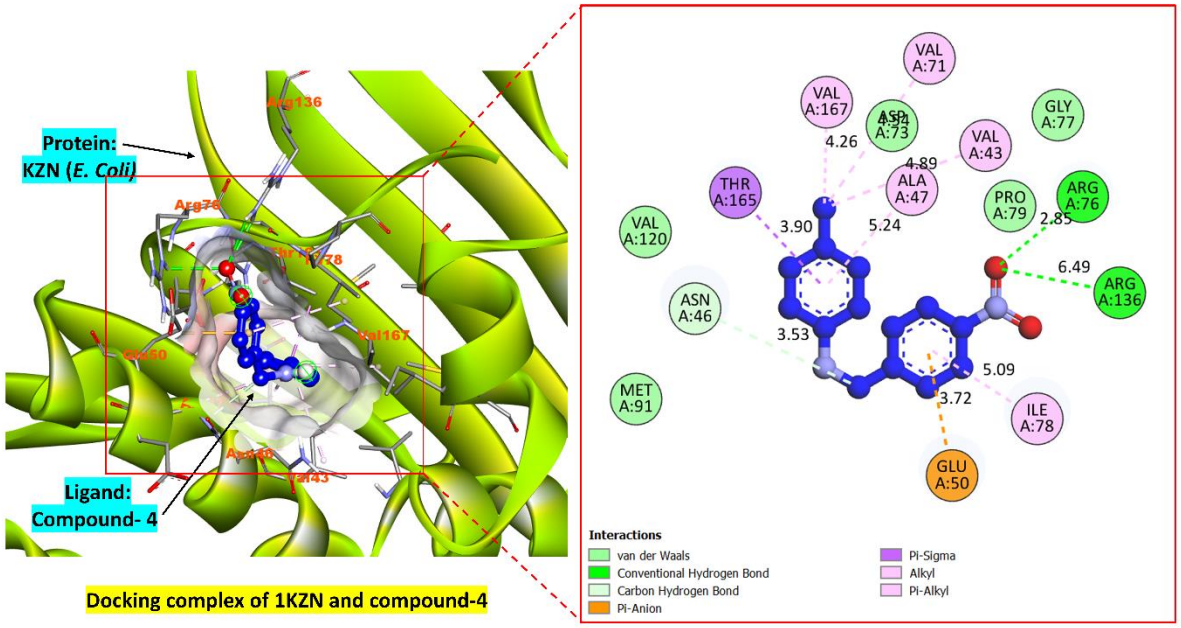

Figure 6: Binding of compound-4 with a target protein 1KZN: Binding cavity and binding interactions.

4.4 *In-silico* ADME properties

The in-silico ADME (Absorption, Distribution, Metabolism, and Excretion) properties of compounds 3 and 4 are summarized in **Tables 3** and **4**. Both compounds possess favorable physicochemical characteristics, suggesting good drug-like potential. Compound 3 ($C_{14}H_{12}N_2O_2$) has a molecular weight of 240.26 g/mol, whereas Compound 4 ($C_{14}H_{14}N_2O_2$) has a molecular weight of 242.27 g/mol, with both values remaining well below the recommended Lipinski threshold of 500 g/mol. Compound 3 contains three hydrogen bond acceptors and no hydrogen bond donors, while Compound 4 possesses two hydrogen bond acceptors and one hydrogen bond donor. The calculated topological polar surface area (TPSA) values were 58.18 $Å^2$ for Compound 3 and 57.85 $Å^2$ for Compound 4, indicating favorable molecular polarity that supports efficient membrane permeability.

Table 3: Pharmacokinetic properties of compounds.

Molecule	Formula	MW	#H-bond acceptors	#H-bond donors	TPSA
compound-3	$C_{14}H_{12}N_2O_2$	240.26	3	0	58.18
compound-4	$C_{14}H_{14}N_2O_2$	242.27	2	1	57.85

Table 4: ADME properties of synthesized compounds.

Molecule	Formula	GI absorption	BBB permeant	Pgp substrate	Lipinski #violations	Bioavailability Score
compound-3	$C_{14}H_{12}N_2O_2$	High	Yes	No	0	0.55
compound-4	$C_{14}H_{14}N_2O_2$	High	Yes	No	0	0.55

The pharmacokinetic prediction revealed that both compounds exhibit high gastrointestinal (GI) absorption, suggesting good oral absorption following administration. Furthermore, both analogues were predicted to be blood–brain barrier (BBB) permeant, indicating their ability to penetrate the central nervous system (**Table 4**)[29, 34] Neither compound was identified as a P-glycoprotein (P-gp) substrate, implying that they are less likely to undergo P-gp-mediated efflux, which may contribute to improved intracellular retention and oral bioavailability. Both compounds also complied with Lipinski's rule of five, exhibiting zero rule violations, thereby supporting their drug-likeness and suitability for oral administration. In addition, each compound showed a bioavailability score of 0.55, indicating moderate oral bioavailability and favorable pharmacokinetic characteristics. Overall, the predicted ADME profile suggests that Compounds 3 and 4 possess promising drug-like properties, making them suitable candidates for further biological evaluation.

4.5 *In-silico* toxicity

The predicted acute oral toxicity of the synthesized compounds was evaluated using the median lethal dose (LD_{50}), expressed in mg/kg body weight, according to the Globally Harmonized System (GHS) for the Classification and Labelling of Chemicals.[35] Compound **3** exhibited a predicted LD_{50} value of 3500 mg/kg, placing it in GHS Toxicity Class V, indicating that it may be harmful if swallowed and suggesting relatively low acute toxicity (**Figure 7**). In contrast, compound **4** showed a predicted LD_{50} value of 400 mg/kg, which falls under GHS Toxicity Class IV, indicating that it is harmful if swallowed and possesses comparatively higher acute toxicity than compound 3.

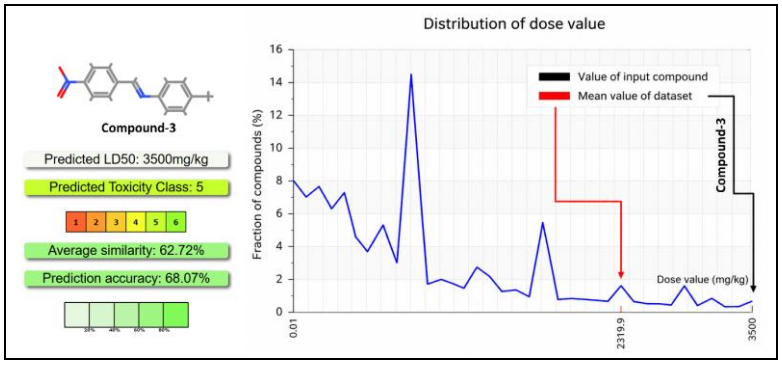

Figure 7: Predicted LD50 value and toxicity class for compound 3.

Overall, the toxicity prediction suggests that compound 3 has a more favorable safety profile with lower acute oral toxicity, whereas compound 4 should be handled with greater caution due to its relatively lower LD_{50} value (**Figure 8**). These in silico toxicity predictions provide

preliminary safety insights and support the selection of compounds for further biological evaluation while highlighting the need for subsequent experimental toxicity studies to validate the computational findings.

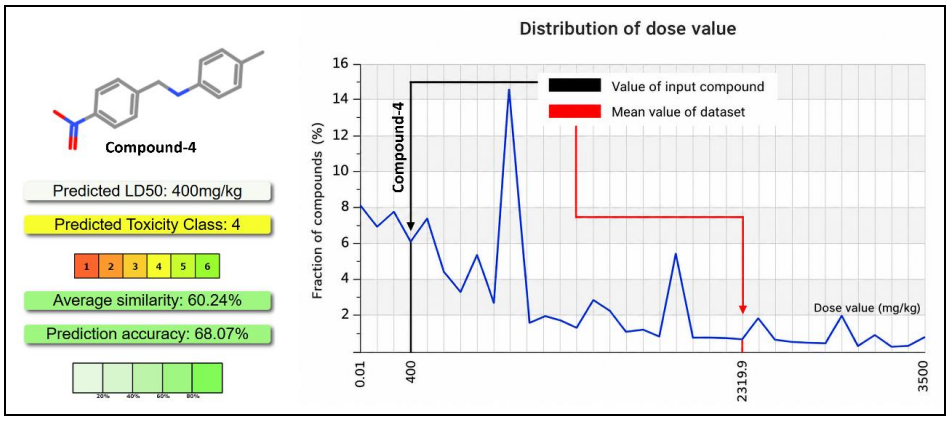

Figure 8: Predicted LD50 value and toxicity class for compound 4.

The in-silico toxicity assessment of the synthesized compounds **3** and **4** revealed an overall acceptable toxicity profile with a few predicted toxicological alerts (**Table 5**). Regarding organ toxicity, compound **3** was predicted to exhibit hepatotoxicity (probability = 0.50) and cardiotoxicity (0.62), whereas compound **4** was predicted to be inactive for hepatotoxicity (0.60) but active for cardiotoxicity (0.56). Both compounds were predicted to be inactive for neurotoxicity, nephrotoxicity, and respiratory toxicity, indicating a lower risk of toxicity toward these organs.

Table 5: In silico toxicity of synthesized compounds.

Classification	Target	Compound-3		Compound-4	
		Prediction	Probability	Prediction	Probability
Organ toxicity	Hepatotoxicity	Active	0.50	Inactive	0.60
	Neurotoxicity	Inactive	0.63	Inactive	0.61
	Nephrotoxicity	Inactive	0.73	Inactive	0.7
	Respiratory toxicity	Inactive	0.71	Inactive	0.50
	Cardiotoxicity	Active	0.62	Active	0.56
Toxicity end points	Carcinogenicity	Active	0.50	Inactive	0.52
	Immunotoxicity	Inactive	0.98	Inactive	0.99
	Mutagenicity	Active	0.77	Active	0.70
	Cytotoxicity	Inactive	0.73	Inactive	0.71
	BBB-barrier	Active	0.87	Active	0.86
	Ecotoxicity	Active	0.82	Active	0.79
	Clinical toxicity	Inactive	0.72	Inactive	0.71
	Nutritional toxicity	Inactive	0.82	Inactive	0.65
Metabolism	Cytochrome CYP1A2	Inactive	0.61	Inactive	0.67
	Cytochrome CYP2C19	Active	0.54	Active	0.60

	Cytochrome CYP2C9	Inactive	0.56	Inactive	0.50
	Cytochrome CYP2D6	Inactive	0.70	Inactive	0.63
	Cytochrome CYP3A4	Inactive	0.54	Inactive	0.50
	Cytochrome CYP2E1	Inactive	0.99	Inactive	0.99

Evaluation of toxicity endpoints showed that compound **3** was predicted to be carcinogenic (0.50), mutagenic (0.77), blood–brain barrier (BBB) permeable (0.87), and ecotoxic (0.82), while remaining inactive for immunotoxicity, cytotoxicity, clinical toxicity, and nutritional toxicity. In comparison, compound **4** was predicted to be non-carcinogenic, but exhibited mutagenicity (0.70), BBB permeability (0.86), and ecotoxicity (0.79), with no predicted immunotoxicity, cytotoxicity, clinical toxicity, or nutritional toxicity. Metabolic toxicity prediction indicated that both compounds were inactive toward CYP1A2, CYP2C9, CYP2D6, CYP3A4, and CYP2E1, while both were predicted to interact with CYP2C19, suggesting a possible influence on CYP2C19-mediated metabolism. Overall, compound **4** demonstrated a comparatively more favorable toxicity profile than compound **3**, primarily due to the absence of predicted hepatotoxicity and carcinogenicity, although both compounds require further experimental toxicological evaluation to validate these computational predictions.

5. CONCLUSION

In the present investigation, two compounds, 4-methyl-N-(4-nitrobenzylidene)aniline (**3**) and 4-methyl-N-(4-nitrobenzyl)aniline (**4**), were successfully synthesized in good yields. Title compounds were produced through an efficient synthetic approach by the synthesis and reduction of the Schiff base. Molecular docking studies against the target protein with PDB ID: 1KZN (*E. coli*) demonstrated favorable binding interactions with active-site residues, indicating good binding affinity (docking scores of -7.7 and -7.4 kcal/mol). Both compounds displayed broad-spectrum antibacterial activity with moderate to good inhibitory effects compared to ciprofloxacin (16–30 mm). Compound **3** showed good antibacterial potency compared to compound 4, particularly against *S. aureus* (24 mm) and *K. pneumoniae* (20 mm). ADME prediction revealed favorable pharmacokinetic profiles for both compounds, including high gastrointestinal absorption, BBB permeability, non-substrate behavior toward P-glycoprotein. Also, zero Lipinski rule violations, favorable toxicity and a bioavailability score of 0.55, suggested good oral drug-likeness. Overall, both compounds exhibited promising antibacterial activity, favorable binding interactions, and desirable

pharmacokinetic and toxicity properties, thus representing promising scaffolds for further study and biological evaluation.

6. REFERENCES

1. I. Mushtaq, M. Ahmad, M. Saleem, and A. Ahmed, "Pharmaceutical significance of Schiff bases: an overview," Future *Journal of Pharmaceutical Sciences*, 1, Feb. 2024; 10; doi: 10.1186/s43094-024-00594-5.
2. D. Gupta, D. P. Pathak, G. Kapoor, and R. Bhutani, "A Comprehensive Review on Synthesis and Biological Activity of Schiff Bases," International *Research Journal of Pharmacy*, June 2019; 10(5): 1–8, doi: 10.7897/2230-8407.1005153.
3. Md. H. Islam and A. Hannan, "Schiff Bases: Contemporary Synthesis, Properties, and Applications," in *Intech Open e Books*, Intech Open, 2024. doi: 10.5772/intechopen.114850.
4. B. Sellami, I. Yamari, and S. Chtita, "Exploration of Schiff Bases: Structures, Syntheses, and Biological Activities," Mini-*Reviews in Medicinal Chemistry*, Mar. 2026; 26: doi: 10.2174/0113895575420281260116222032.
5. S. D. Madaboina and G. Kamala, "Structure, Biological Activities and Synthesis of Schiff Bases," Journal *of Pharma Insights and Research.*, Aug. 2025; 3(4): 94–101. doi: 10.69613/h48ev841.
6. T. Akitsu, Schiff *Base in Organic, Inorganic and Physical Chemistry.* Intech Open, 2022. doi: 10.5772/intechopen.104134.
7. M. S. Sinicropi et al., "Metal Complexes with Schiff Bases: Data Collection and Recent Studies on Biological Activities," International *Journal of Molecular Sciences*, Nov. 2022; 23(23): 14840–14840, doi: 10.3390/ijms232314840.
8. S. K. Raju, A. Settu, A. Thiyagarajan, D. Rama, P. Sekar, and S. Kumar, "Biological applications of Schiff bases: An overview," GSC *Biological and Pharmaceutical Sciences*, Dec. 2022; 21(3): 203–215, doi: 10.30574/gscbps.2022.21.3.0484.
9. S. N. Bhavsar, "Literature Review on Schiff Bases," 2024; 73–82. doi: 10.58532/v3becm2ch5.
10. I. E. Otuokere et al., "Biological Potentials of Some Schiff Bases and Their Chelates: A Short Review," *Intech Open eBooks*, Aug. 2024, doi: 10.5772/intechopen.114862.
11. S. A. D. - and D. S. chourisia -, "Overview of Biological Activities and Synthesis of Schiff Base," *International Journal for Multidisciplinary Research*, Aug. 2024; 6(4): doi: 10.36948/ijfmr.2024.v06i04.26078.

12. R. Shivhare *et al.*, "Schiff Base as Multifaceted Bioactive Core," in IntechOpen *eBooks*, Intech Open, 2022. doi: 10.5772/intechopen.108387.
13. H. A. Dahlawi and M. Asif, "Pharmacological Potential and Biological Applications of Various Schiff Base Analogues," Russian *Journal of Organic Chemistry*, Dec. 2025; 61(12): 2367–2390, doi: 10.1134/s1070428025601554.
14. A. Abd-El-Aziz et al., "Advances in Coordination Chemistry of Schiff Base Complexes: A Journey from Nanoarchitectonic Design to Biomedical Applications," Topics *in Current Chemistry*, Feb. 2025; 383(1): 8–8, doi: 10.1007/s41061-025-00489-w.
15. A. Ullah and K. S. Bukhari, "Exploring Recent Advancements in Schiff Base Chemistry," in Contact-*less Assessment of In-vivo Body Signals Using Microwave Doppler Radar (InTech)*, Intech (Slovakia), 2024. doi: 10.5772/intechopen.114004.
16. A. Soroceanu and A. Bargan, "Advanced and Biomedical Applications of Schiff-Base Ligands and Their Metal Complexes: A Review," *Crystals*, Oct. 2022; 12(10): 1436–1436, doi: 10.3390/cryst12101436.
17. A. A. Hamad, R. A. Omer, K. N. Kaka, E. I. Abdulkareem, and R. F. Rashid, "Biological activities of metal complexes with Schiff base," Reviews *in Inorganic Chemistry*, Oct. 2024; 45(3): 543–552, doi: 10.1515/revic-2024-0075.
18. N. Yadav, S. Chauhan, S. Sangwan, R. Kumar, and S. Deepak, "Recent Advances in Anti-Urease Activity of Schiff Bases and their Metal Complexes," Asian *Journal of Chemistry*, Mar. 2024; 36(4): 779–794, Mar. 2024, doi: 10.14233/ajchem.2024.31333.
19. S. Kumar et al., "Advances in chromone-based copper(ii) Schiff base complexes: synthesis, characterization, and versatile applications in pharmacology and biomimetic catalysis," RSC *Advances*, Jan. 2024; 14(24): 17102–17139, doi: 10.1039/d4ra00590b.
20. S. K. Raju, A. Settu, A. Thiyagarajan, D. Rama, P. Sekar, and S. Kumar, "Synthetic approaches of medicinally important Schiff bases: An updated Review," World *Journal of Advanced Research and Reviews*, Dec. 2022; 16(3): 838–852, doi: 10.30574/wjarr.2022.16.3.1394.
21. X. Liu and J. Hamon, "Recent developments in penta-, hexa- and heptadentate Schiff base ligands and their metal complexes," Coordination *Chemistry Reviews*, Mar. 2019; 389: 94–118, doi: 10.1016/j.ccr.2019.03.010.
22. L. A. Barreras-Contreras et al., "Schiff Bases and Metal Complexes as Multifunctional Platforms: Bridging Bioinorganic Chemistry, Catalysis, Sensing, and Energy Applications," *Bioinorganic Chemistry and Applications*, Jan. 2025; 1: 8829417–8829417, doi: 10.1155/bca/8829417.

23. N. T. Subaşı, "A Comprehensive Review on Schiff Bases: Development Process, Green Synthetic Strategies, and Versatile Applications," in *IntechOpen eBooks*, Intech Open, 2025. doi: 10.5772/intechopen.1012219.
24. S. Nagar, S. Raizada, and N. Tripathee, "A review on various green methods for synthesis of Schiff base ligands and their metal complexes," *Results in Chemistry*, Oct. 2023; 6: 101153–101153, doi: 10.1016/j.rechem.2023.101153.
25. V. R. Kaulić, N. P. Juraj, B. Perić, Z. Štefanić, S. I. Kirin, and S. Raić-Malić, "Transition Metal-Mediated Hydrolysis of the Imine Bond in 2-Azomethine Benzothiazoles," *Croatica Chemica Acta*, Jan. 2023; 95(4): 123–130, doi: 10.5562/cca3907.
26. A. Beillard, X. Bantreil, T. Métro, J. Martínez, and F. Lamaty, "Alternative Technologies That Facilitate Access to Discrete Metal Complexes," *Chemical Reviews*, May 2019; 119(12): 7529–7609, doi: 10.1021/acs.chemrev.8b00479.
27. M. A. Malik, O. A. Dar, P. Gull, M. Y. Wani, and A. A. Hashmi, "Heterocyclic Schiff base transition metal complexes in antimicrobial and anticancer chemotherapy," *Med Chem Comm.*, Dec. 2017; 9(3): 409–436, doi: 10.1039/c7md00526a.
28. T. Bhattacharjee *et al.*, "Syntheses, crystal structures, theoretical studies, and anticancer properties of an unsymmetrical schiff base ligand N-2-(6-methylpyridyl)-2-hydroxy-1-naphthaldimine and its Ni(II) complex," *Journal of Molecular Structure*, July 2022; 1269: 133717–133717, doi: 10.1016/j.molstruc.2022.133717.
29. S. R. Jadhav, S. S. Gurav, H. Yasin, and P. Nagpal, "Imidazo [1 , 2-a] pyridine-appended chalcone and Schiff base conjugates : Synthetic, spectrophotometric, biological, and computational aspects," *Chem. Phys. Impact*, 9: July 2024; 100694. doi: 10.1016/j.chphi.2024.100694.
30. M. Kurbanova, F. Gurbanova, H. Yasin, S. S. Gurav, and C. Lai, "Synthesis, structure, DFT study and molecular docking inspection of spirobi [hexahydropyrimidine] -diones derivative," *Chem. Phys. Impact*, 9: August 2024; 100716, doi: 10.1016/j.chphi.2024.100716.
31. K. B. Gangurde *et al.*, "Thiazole derivatives as promising antimicrobial and antioxidant agents : insights from synthesis, bioactivity, and computational studies," *J. Sul. Chem.* 2025. doi: 10.1080/17415993.2025.2488851.
32. S. V Raskar, K. T. Waghmode, and S. S. Gurav, "Synthesis, Characterization, Molecular Docking, and DFT Methanone Derivatives," *J. Comput. Biophys. Chem.*, 2026; 25: 415–430. doi: 10.1142/S2737416525500528.

33. S. S. Gurav, S. R. Jadhav, O. A. Lotlikar, and K. T. Waghmode, "An efficient one-pot multicomponent, Amberlite IR120 (H) catalyzed microwave-assisted synthesis mechanism and antibacterial evaluation," *Synth. Commun.*, 2023; 53(23): 2029–2040 doi: 10.1080/00397911.2023.2267131.
34. O. A. Lotlikar *et al.*, "Green Chemistry Letters and Reviews Microwave and ultrasound-assisted green protocols for 5-methylthiazole induced Betti bases : molecular docking, in-silico pharmacokinetics , and anticancer activity studies," *Green Chem. Lett. Rev.*, 2024; 1–15. doi: 10.1080/17518253.2024.2403608.
35. N. Kumar, H. Yasin, S. Sharma, and S. S. Gurav, "Studies on chlorophenyl , thiophenyl, and biphenyl clubbed tetrahydro bipyrazole carbaldehydes: Synthesis, antimicrobial and antioxidant activity, SAR study, in-silico pharmacokinetics, toxicity, and molecular modeling," *Chem. Phys. Impact*, 9: August 2024; 100713. doi: 10.1016/j.chphi.2024.100713.